BULLETIN OF THE POLISH ACADEMY OF SCIENCES
TECHNICAL SCIENCES
Vol. 52, No. 4, 2004

Microstructural refinement and properties of metals processed by severe plastic deformation

K. J. KURZYDŁOWSKI*

Faculty of Materials Science and Engineering, Warsaw University of Technology, 141 Woloska St., 02–507 Warsaw, Poland

Abstract. This paper presents the results obtained from the structural refinement of selected metals and alloys produced by severe plastic deformation processes. Large levels of deformations were produced using four methods, which differed in the character and dynamics of the loading, as well as in the intensity and homogeneity of the plastic strain field. Qualitative and quantitative studies of the refined microstructure were carried out using stereological and computer image analytical methods. Microhardness and selected mechanical properties, such as strength and yield point, were also determined.

Keywords: severe plastic deformation, nanometals, multi-scale structure.

1. Introduction

In recent years, a number of methods for refining the structure of metals by severe plastic deformation (SDP) have been developed. Some of those methods permit grain refinement to a nanometric level. Numerous investigations show that the metals having such a structure are characterized by a number of specific properties including significantly higher yield point than that produced by conventional deformation methods (rolling, drawing).

At the same time, the mechanical properties of these SPD materials exhibit a large scatter.

The aim of this paper is to investigate the microstructure of metallic materials produced by SPD and the relationships between the mechanical properties of commonly used metallic materials and the deformation routes.

2. Materials and methodology used

Different SPD process were used on specimens of 316L steel, iron, copper, aluminum, and titanium. Specimens of these materials were subjected to severe plastic deformation using the following methods:

— equal channel angular pressing (ECAP)
— hydrostatic extrusion (HE)
— high pressure torsion (HPT)
— Max-Strain cumulative plastic deformation by a varying path (MS)

Cylindrical specimens of diameter 20mm were deformed by ECAP using the system shown schematically in Fig. 1.

The specimens were rotated 180° around the longitudinal axis before each cycle of pressing through the channel. The material was subjected to 12 cycles, which enabled a total true deformation of 13.8. to be obtained [1].

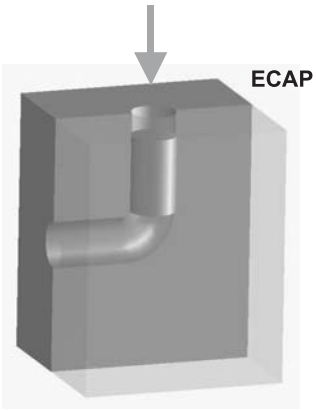

Fig. 1. Scheme of the ECAP process

The principles of hydrostatic extrusion are shown in Fig. 2. A billet of the test material is extruded through a die, located in the operational chamber.

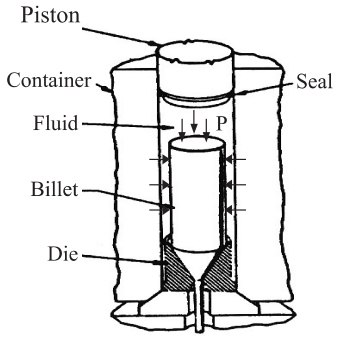

Fig. 2. Principles of hydrostatic extrusion

During the hydrostatic extrusion process the piston does not contact the charge material and in the deformation zone of the die (the cone) the material itself flows on a film of lubricant under the applied pressure (hydrodynamic lubrication). Very low friction allows for severe deformations in the range of 2.0, [2].

* e-mail: kjk@inmat.pw.edu.pl

The HPT method consists of simultaneous compression and torsional deformation of the specimen as shown schematically in Fig. 3. Typical HPT specimens are in the form of a disc sample (for this work 10mm in diameter and 0,3mm thick). After 5 rotations of the cupping punch the plastic deformation amounts to 12.

Fig. 3. Scheme of the HPT process

Large Plastic Deformations were also achieved using Max Strain unit. This Unit allows the deformation to be controlled via cyclic compression in 3 perpendicular directions [3].

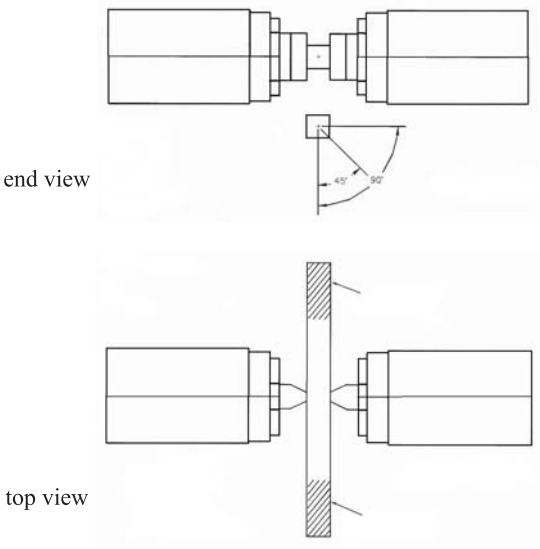

Fig. 4. Schematic explanation of the deformation of Max Strain system

In the present study the specimens were deformed in a Gleeble 3800 simulator. The deformation rate was 1 s^{-1}. A schematic explanation of deformation by the Max Strain system is shown in Fig. 4. All specimens were deformed to the logarithmic true strain value $\varepsilon_c = 40$ (one cycle strain = 0.2; 200 cycles) at temperature of $0{,}33T_m$ where T_m is the melting point of the particular material.

3. Microstructural examination

The microstructures of the deformed materials, obtained by these methods, were investigated by transmission (TEM) and scanning (SEM) electron microscope and, in some cases, light microscopy. The findings of the investigations are briefly discussed below.

3.1. ECAP. An image of the microstructure of iron subjected to ECAP is shown in Fig. 5. The Characteristic feature of this material is a banded microstructure which renders the ECAP blanks macroscopically inhomogeneous.

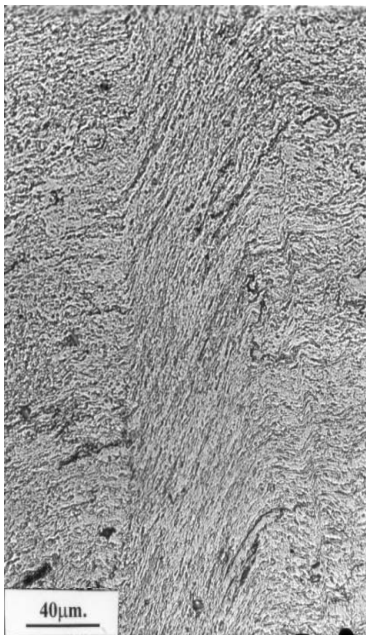

Fig. 5. Banding microstructure in ECAP iron

Under higher magnification submicroscopic bands can be identified inside the microscopic observed bands. This proved that the banding structures develop in multi length scales during the ECAP processing.

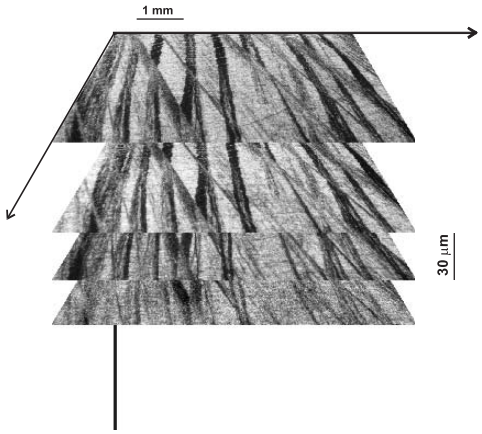

Fig. 6. Serial sections of ECAP Fe specimen

The macroscopic bands on average account for 50% of the iron volume. From this point of view ECAP iron can be considered as possessing a laminated structure. The spatial arrangement of the bands, have been studied by serial sectioning of specimens. [4]

Figure 6 shows images on successive section which clearly indicating that the bands change their spatial orientation.

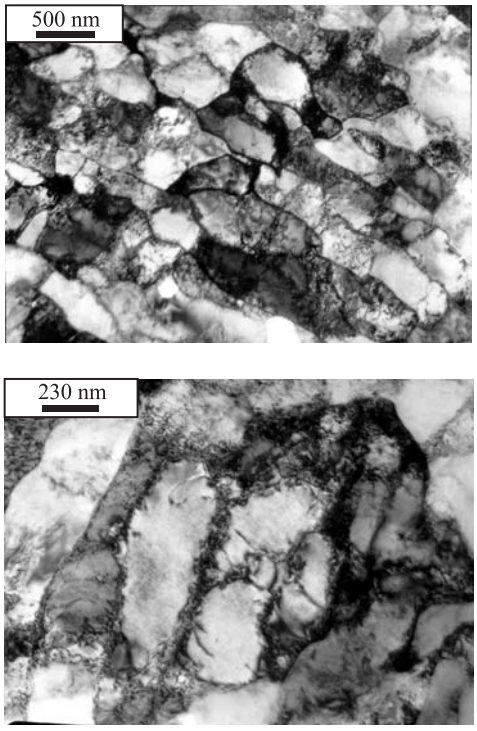

Fig. 7. TEM images of the microstructure of ECAP iron

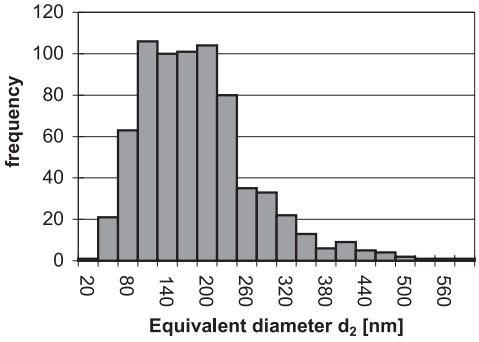

Fig. 8. Diameters distribution of ECAP iron

TEM images of ECAP iron are shown in Fig. 7. Measurements of grain size reveal an average equivalent diameter, $E(d_2)$, of 170 nm. However, the histogram, Figure 8, shows that a large portion of the grains have a size below 140 nm.

The grains observed by TEM are characterized by two types of spatial arrangement: random and orientated. It can be concluded that an orientated microstructure exists within the bands while the surrounding matrix contains grains with random orientation of the elongation axis. TEM studies of the ECAP iron also proved that a large number of grain boundaries are characterized by a high angle of misorientation as shown in Fig. 9 (the misorientation has been measured using special software [5]).

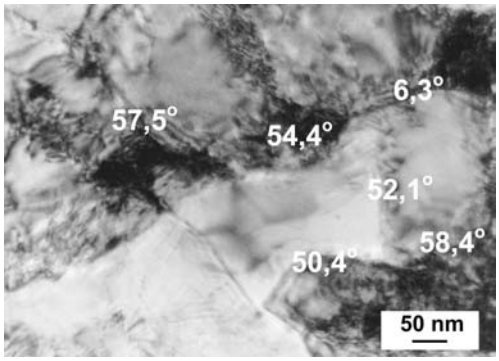

Fig. 9. Grain misorientation for ECAP iron

3.2. HE. The microstructures of 316 L austenitic stainless steel subjected to HE is illustrated in Fig. 10. In the longitudinal sections a "fibre" type structure is observed at low magnification.

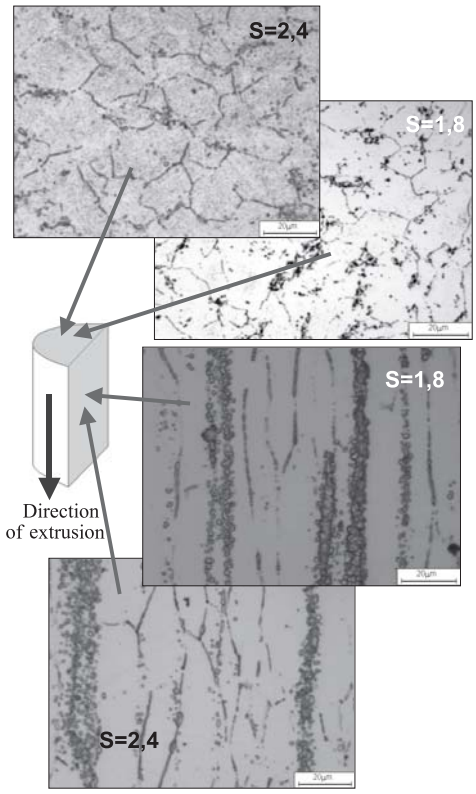

Fig. 10. Microstructure of steel 316L after hydroextrusion (light microscopy)

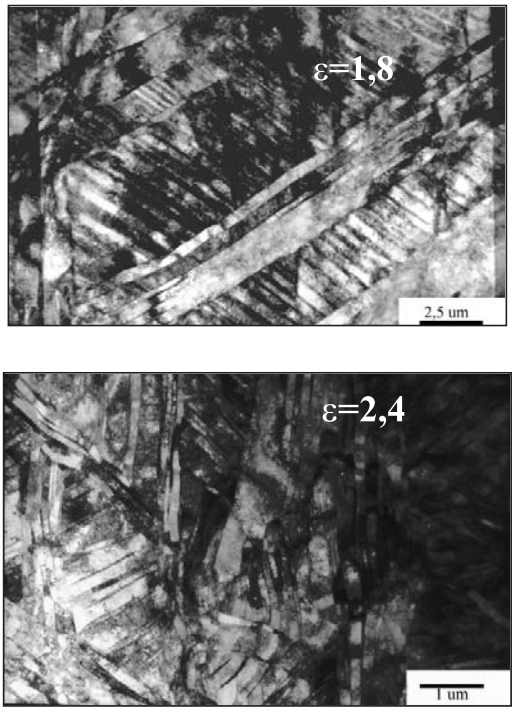

Fig. 11. TEM images of the microstructure of steel 316L after hydroextrusion process, average thickness of twins is 300 nm

TEM revealed deformation twins in the primary austenite (Fig. 11). These twins intersect at various angles forming characteristic block — structure on a nanometric scale.

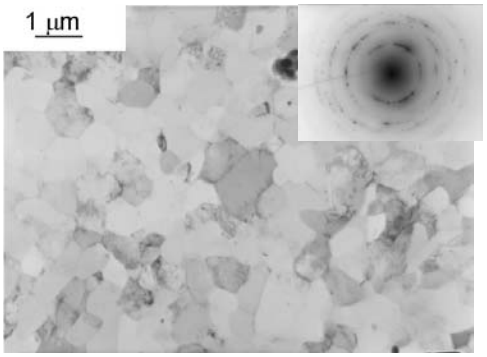

Fig. 12. TEM image Al subjected to hydrostatic extrusion (true strain 3,5)

In the case of aluminum subjected to hydrostatic extrusion, TEM examination revealed a fairly homogenous structure consisting of grains free of dislocations as shown in Fig. 12. The selected area electron diffraction (SAED) pattern exhibits an image which indicates that the microstructure consists of grains separated by high angle boundaries. This has been further confirmed by direct measurement of the misorientation.

The microstructure of the titanium after hydrostatic extrusion is presented in Fig. 13. Grain size measurements have shown that mean equivalent diameter of grains sharply decreases with increasing strain. An average grain size of 90 nm has been obtained after applying a cumulative true strain of 3.82.

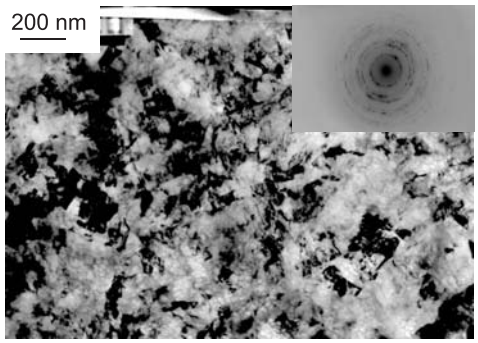

Fig. 13. The microstructure of Ti after HE (true strain 3.8)

3.3. HPT. Light microscopy and TEM of the iron microstructure subjected to HPT are presented in Figs. 14 and 15 respectively. Concentric circles on the specimen surface are made by the rotating punch. Rings on HPT iron appear on the entire surface except at the centre of about 1 mm diameter. Some details of the structure of these rings are illustrated by the image in Fig. 14 which shows the area half a diameter distant from the centre. The presence of rings indicates macroscopic nonhomogeneity of HPT steel and axial (rotational) symmetry.

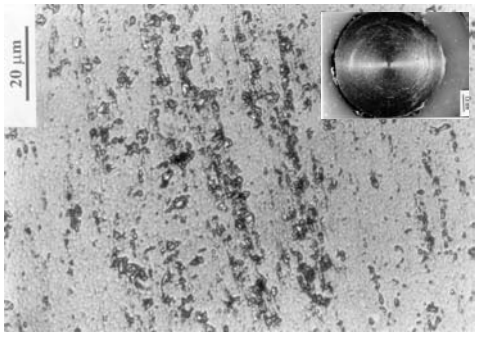

Fig. 14. The metallographic specimen of the iron specimen after HPT (light microscopy)

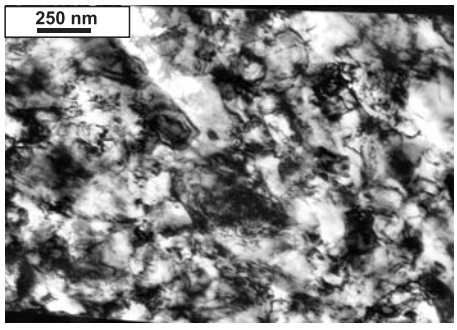

Fig. 15. Iron microstructure after HPT

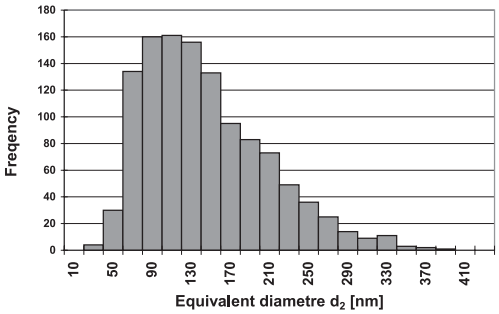

Fig. 16. Distribution of diameter of HPT iron

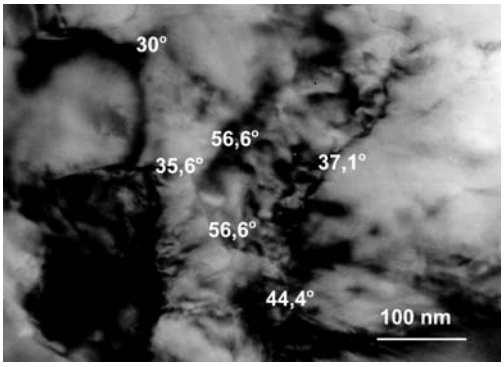

Fig. 17. Grain misorientation for HPT subjected iron

Figure 15 shows the TEM image of the microstructure of iron subjected to HPT. The microstructure is characterized by a relatively homogenous size of dislocation-free areas of average size $E(d_2) = 134$ nm with the majority in the range 90–170 nm (see Fig. 16). It should also be noted that the number of sharply outlined grain boundaries in the material, which are typical of materials having high angle disorientations, is relatively low (see also Fig. 17).

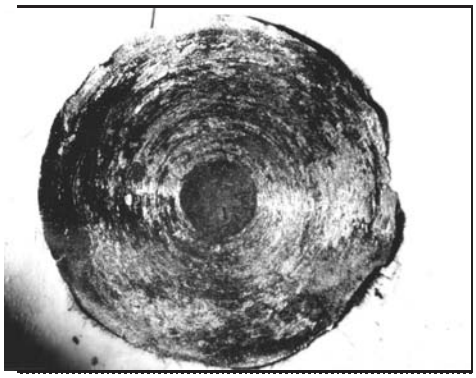

Fig. 18. 316 L Steel after HPT

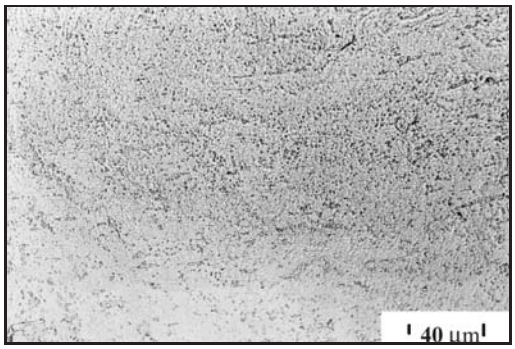

Fig. 19. Microstructure at the center of the 316L steel after HPT

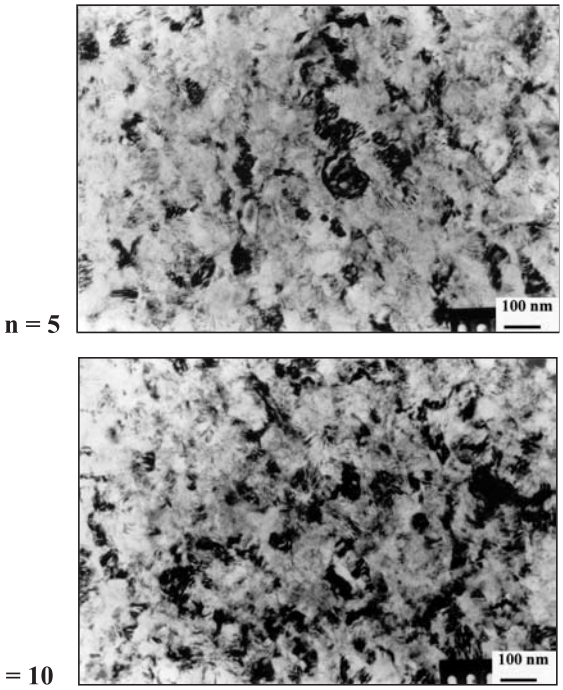

Fig. 20. TEM images of the microstructures of 316L steel subjected to 5 and 10 rotations

Light microscopy observations of the microstructure of 316L steel confirm the non-homogeneous nature of the structure obtained by HPT (Fig. 18). A more homogeneous structure is observed in the center of the specimens, as shown in the microphotography in Fig. 19.

Figure 20 shows that microstructure in the deformed part of the HPT specimen is already significantly refined after 5 rotations. An additional 5 rotations causes only a small decrease in the size of dislocations of free grains. [6, 7]

3.4. Max Strain. Plastic deformation carried out by cumulative plastic deformation was applied to aluminum alloy PA6, copper, iron and austenitic steel 316L using a Max Strain unit of the Gleeble system. Figure 21 shows the copper specimen after deformation. The areas used for microstructural examination are indicated.

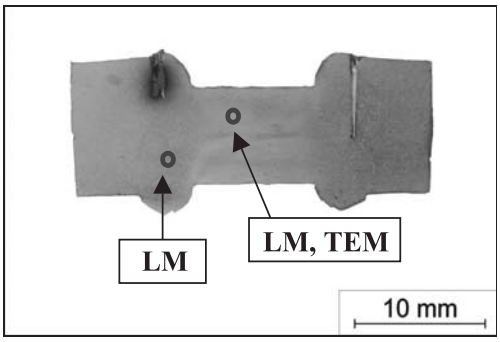

Fig. 21. Cu specimen after Max Strain process

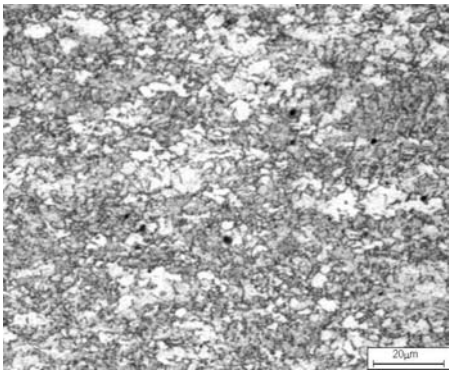

Fig. 22. Microstructure of the center area of the copper specimen after Max Strain

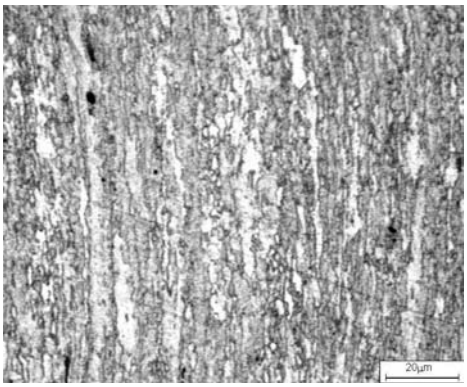

Fig. 23. Microstructure of the edge area of the deformed fragment of the copper specimen after Max Strain

The microstructure from the central area of the copper specimens reveal large grain size refinement and homogeneity, as shown in Fig. 22. The microstructure at the edge (Fig. 23) reveals a higher average grain size and grain elongation.

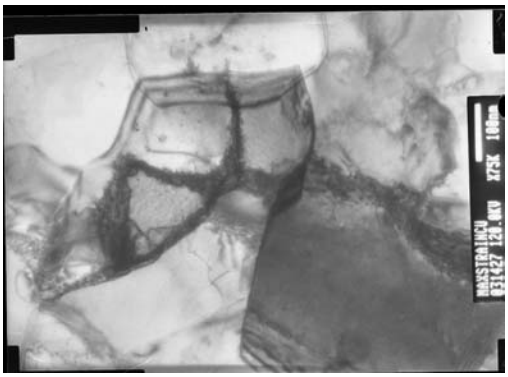

Fig. 24. TEM image of the Cu microstructure after Max Strain process

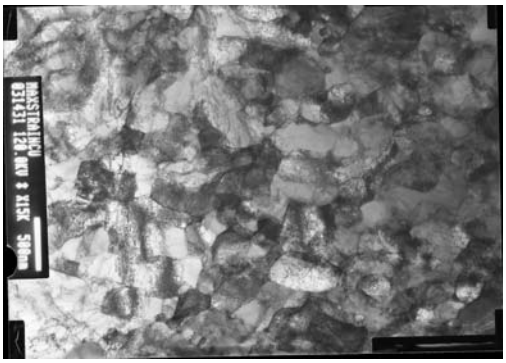

Fig. 25. TEM image of the Cu microstructure after Max Strain process

TEM images form the center are presented in Figs. 24 and 25. Similar images for iron are shown in Figs. 26–30.

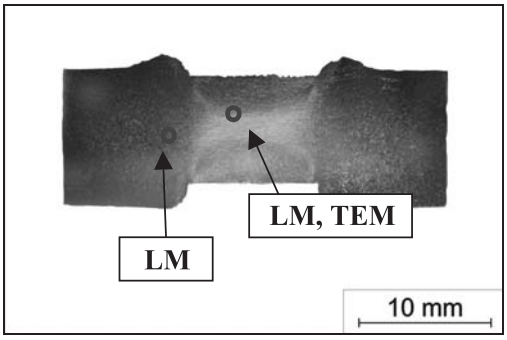

Fig. 26. Image of the iron specimen after Max Strain process and the areas of the microstructure examinations

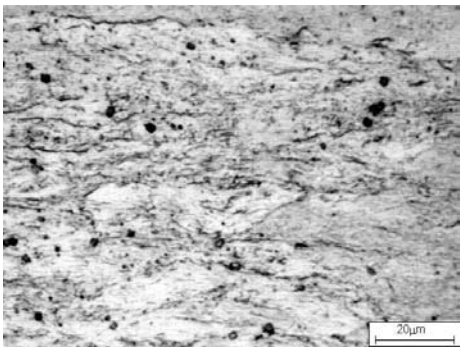

Fig. 27. Microstructure of the iron after Max Strain obtained from the center of the deformed specimen

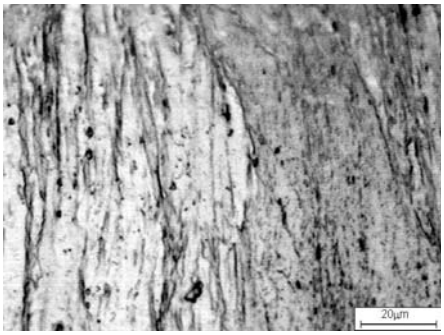

Fig. 28. Microstructure of the iron after Max Strain obtained at the edge of deformed specimen.

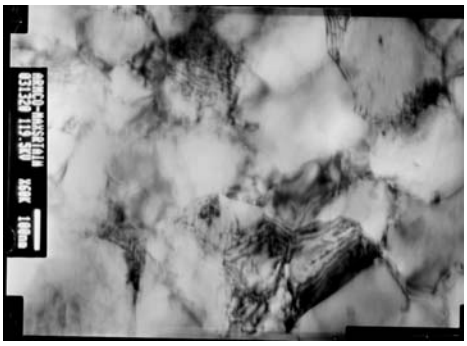

Fig. 29. TEM image of the Fe microstructure after Max Strain process

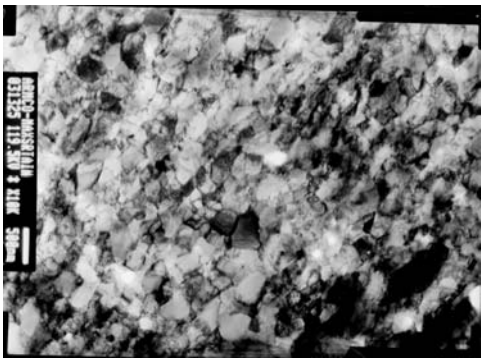

Fig. 30. TEM image of the Fe microstructure

4. Quantifying of microstructures

Images of the microstructure of the specimens subjected to different methods of severe plastic deformation have been used to measure the following parameters:

- $E(d)$ [nm] — average value of the equivalent diameter of dislocation free crystals
- $CV(d_2)$ — variation coefficient of the average equivalent diameter

Table 1
Comparison of the values of $E(d_2)$, $CV(d_2)$ and $E(d_{\max}/d_2)$ parameters for the studied materials

Method of SPD	Parameter materials	Value
	316 L	
	$E(d_2)$ [nm]	**300 nm***
HE	$CV(d_2)$	**0,98**
	$E(d_{\max}/d_2)$	**1,52**
	$E(d_2)$ [nm]	**60 nm**
HPT	$CV(d_2)$	**0,84**
	$E(d_{\max}/d_2)$	**1,31**
	$E(d_2)$ [nm]	**220 nm**
Max Starin	$CV(d_2)$	**0,72**
	$E(d_{\max}/d_2)$	**1,28**
	Fe	
	$E(d_2)$ [nm]	**134 nm**
HPT	$CV(d_2)$	**0,80**
	$E(d_{\max}/d_2)$	**1,28**
	$E(d_2)$ [nm]	**245 nm**
Max Strain	$CV(d_2)$	**0,94**
	$E(\alpha)$	**1,24**
	$E(d)$ [nm]	**171 nm**
ECAP	$CV(d_2)$	**1,03**
	$E(d_{\max}/d_2)$	**1,36**
	Cu	
	$E(d)$ [nm]	**280 nm**
Max Strain	$CV(d_2)$	**0,82**
	$E(d_{\max}/d_2)$	**1,26**
	PA6, Al	
	$E(d)$ [nm]	**700 nm**
HE (Al)	$CV(d_2)$	**0,58**
	$E(d_{\max}/d_2)$	**1,22**
	$E(d)$ [nm]	**296 nm**
Max Strain (PA6)	$CV(d_2)$	**0,68**
	$E(d_{\max}/d_2)$	**1,24**
	Ti	
	$E(d)$ [nm]	**86 nm**
HE	$CV(d_2)$	**0,5**
	$E(d_{\max}/d_2)$	**1,25**

* average thickness of twins

- $E(d_{\max}/d_2)$ — average value of the elongation factor (defined as the ratio of maximum diameter to equivalent diameter), [8].

The results presented in Table 1, show that the largest grain size occurred after hydroextrusion [6]. The smallest grain size was obtained in iron after the HPT process. Relatively low values of $CV(d_2)$ are found in specimens subjected to cumulative plastic deformation.

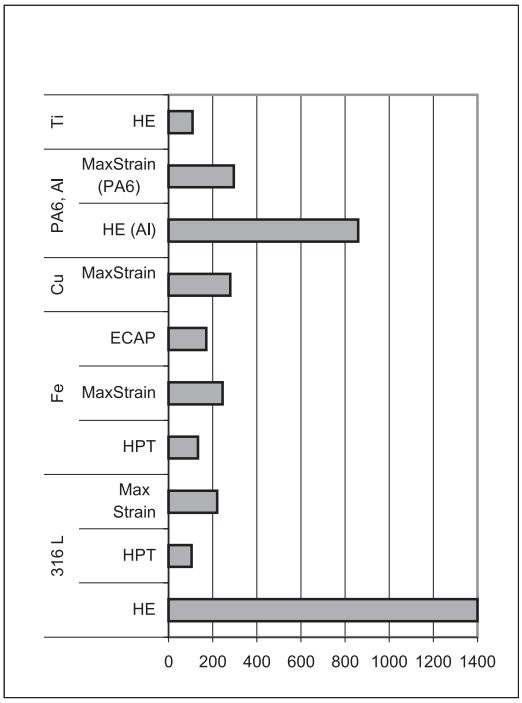

Fig. 31. Average grain size for the materials after different SPD processes

It should be noted that the elongation factor, for all cases, varies in the range 1.22 to 1.52. These values indicate relatively regular geometry of the microstructures obtained by SPD. Differences in the average grain size between the particular materials are given in Fig. 31.

5. Mechanical properties

Mechanical properties of the materials subjected to the different deformation processes were determined, for both transverse and longitudinal sections, by static tensile tests and microhardness.

The tensile tests were performed at room temperature using a QTest/10, manufactured by MTS. The dimensions of the micro- specimens used for tensile testing is shown in Fig. 32. Figure 33 shows the location of specimens.

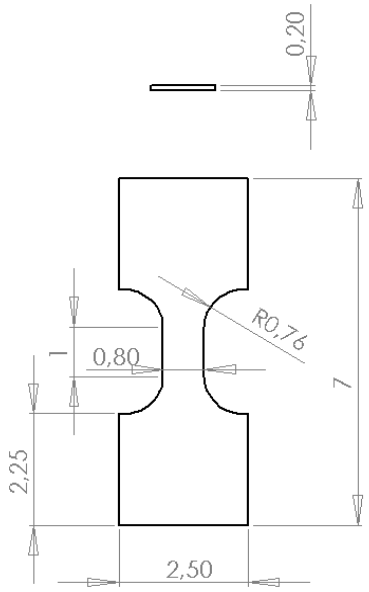

Fig. 32. Dimensions of the micro specimen for tensile tests

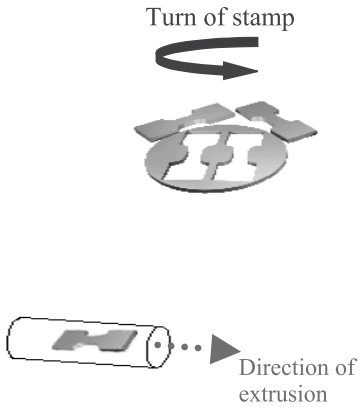

Fig. 33. Schematic explanation of the microspecimens acquisition

Testpieces were produced using an electro-sparking machine to minimise the heat-affected zone. This is important because of the small size of specimens 0.2 mm thick and 0.8 mm wide. [6, 9, 10]

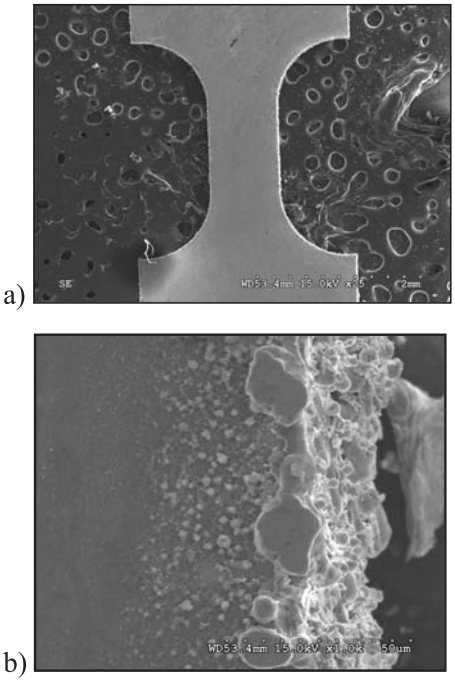

Fig. 34. SEM image of a specimen machined by electro-sparking machine (a) and on the oxides layer at their edge (b)

The SEM image of a machined specimen is given as Fig. 34. The film of oxide visible on the surface of the specimen is about 25 μm thick. Therefore, it can be assumed that the width of the heat-effected zone is of similar size, indicating that the HAZ affects about 6% of the volume.

Microscopic observations of the specimens after tension revealed that cracking of the material occurs in the region of the shoulders (Fig. 35).

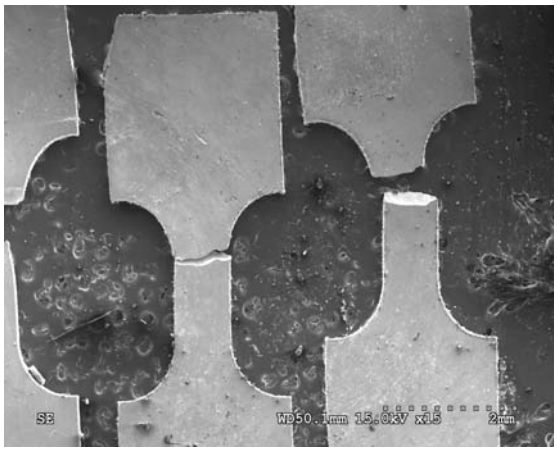

Fig. 35. Microspecimen from a specimen subjected to high pressure torsion (HPT) after tension process (SEM)

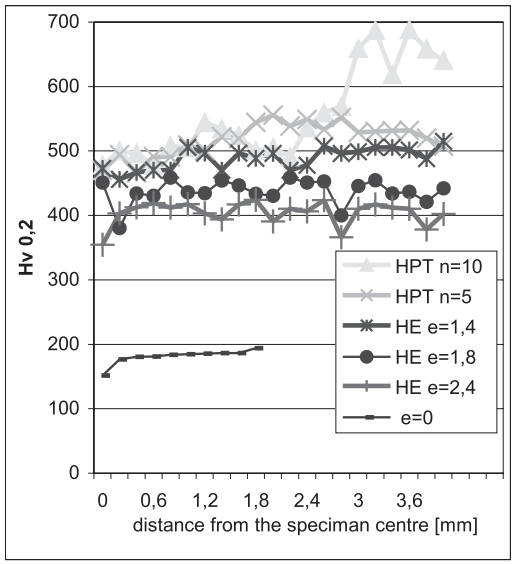

Fig. 36. Microhardness profiles of steel 316L after HE and HPT processes

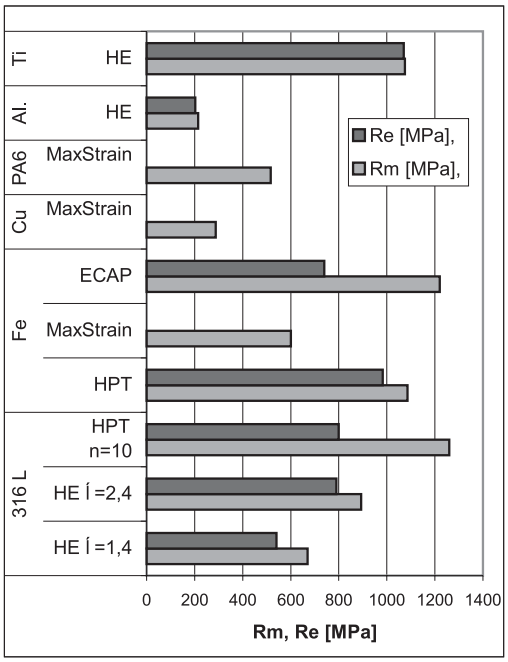

Fig. 37. Yield point and strength of the materials after SPD processes

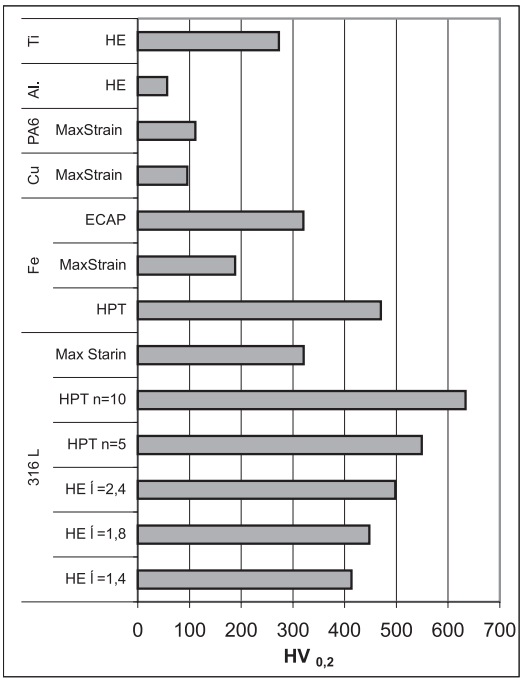

Fig. 38. Average microhardness values for the materials after SPD processes

The fracture surfaces run perpendicularly to the strain direction. Measured values of the yield point and strength are presented in Table 2. The table contains also the average values of microhardness. Profiles of the microhardness were also obtained for the majority of the specimens. Fig. 36 shows microhardness profile of the austenitic steel after hydroextrusion and high pressure torsion (HTP).

Variations in the strength of the examined materials are also illustrated in Fig. 37. Similar diagram for the microhardness is presented in Fig. 38.

6. Discussion and conclusions

The results obtained in the present study show that there are now a number of methods of SPD that can be used to refine the structure of metals.

The microstructures of the materials subjected to severe plastic deformation studied in this work displayed considerable refinement, characterised by the formation of nano-sized crystals. However, the studies also show that severe deformation results in specific method-dependent, macroscopic features. In particular, a characteristic banded microstructure is observed in ECAP and a fibrous structure in HE materials. The observed character of the microstructure is strictly related to the deformation method. The localized deformation bands are particularly characteristic for the near-shear deformation.

The tensile strength of the SPD materials studied in this work increased significantly, and their ductility was preserved. In view of the results obtained on a large number of metals and alloys a conclusion can be drawn that SPD could become an attractive way of processing materials for a variety of applications, i.e. bio-medical [11].

Table 2
Yield point, strength and microhardness for SPD specimens

Method of SPD	Property	Value [Mpa]
	316 L	
HE	R_m [MPa],	
	$\varepsilon = 1.4$	670
	$\varepsilon = 2.4$	893
	R_e [MPa],	
	$\varepsilon = 1.4$	540
	$\varepsilon = 2.4$	790
	$HV_{0,2}$,	
	$\varepsilon = 1.4$	413 ± 20
	$\varepsilon = 1.8$	448 ± 18
	$\varepsilon = 2.4$	498 ± 8
HPT	R_m [MPa]	1260 ± 128
	$R_{0,2}$ [MPa]	800 ± 173
	$HV_{0,2}$	
	$n = 5$	549 ± 23
	$n = 10$	634 ± 49
Max Strain	R_m [MPa]	1080
	R_e [MPa]	950
	$HV_{0,2}$	321 ± 46
	Fe	
HPT	R_m [MPa]	1086
	R_e [MPa]	983
	$HV_{0,2}$	470
Max Strain	R_m [MPa]	600,36
	$HV_{0,2}$	189 ± 22
ECAP	R_m [MPa]	1220
	R_e [MPa]	740
	$HV_{0,2}$	320
	Cu	
Max Strain	R_m [MPa]	288,54
	R_e [MPa]	
	$HV_{0,2}$	97 ± 12
	PA6, Al	
HE (Al)	R_m [MPa]	214
	R_e [MPa]	202
	$HV_{0,2}$	57 ± 2
Max Strain (PA6)	R_m [MPa]	518
	$R_{0,2}$ [MPa]	
	$HV_{0,2}$	111 ± 34
	Ti	
HE	R_m [MPa]	1075
	$R_{0,2}$ [MPa]	1070
	$HV_{0,2}$	273 ± 8

Acknowledgements. This paper makes reference to the results obtained by Małgorzata Suś-Ryszkowska, Anna Drużycka-Wiencek, Halina Garbacz, Malgorzata Lewandowska, Tomasz Wejrzanowski i Dominik Kukla in the project financed by the Polish State Committee for Scientific Research (PBZ-KBN-096/T08/2003) coordinated by the Author).

References

[1] M. Suś-Ryszkowska, T. Wejrzanowski, Z. Pakieła and K. J. Kurzydłowski, "Microstructure of ECAP severely deformed iron and its mechanical properties", *Mat. Sc. Eng.* A369 (204), p. 151.

[2] M. Lewandowska, H. Garbacz, W. Pachla and K. J. Kurzydlowski, "Hydrostatic extrusion and nanostructure formation in an aluminium alloy", *Solid State Phenomena* 101–102, 65–68 (2005).

[3] R. Z. Valiev, "Ultrafinegrained materials produced by severe plastic deformation [special issue]", *Ann. Chim.–Mater. Sc.* 21, 369 (1996).

[4] M. Sus-Ryszkowska, M. Miskiewicz, Z. Pakieła and K. J. Kurzydlowski, "Strain localization in nanocrystalline iron processed by Severe Plastic Deformation", *Solid State Phenomena* 101, 81 (2004).

[5] M. Richert, K. Chruściel, A. Baczmański and J. Długopolski, *MIROANALIZA II — Dezorientacje i Mikrotekstura KILIN 1.21*, Kraków 2002.

[6] Z. Pakieła, M. Miśkiewicz, K. Paradowski, A. Drużycka-Wiencek and K. J Kurzydłowski, "Ductility of nanocrystalline materials processed by severe plastic deformation", *Solid State Phenomena*, (to be published).

[7] Z. Pakieła and M. Suś-Ryszkowska, "Influence of microstructure heterogeneity on the mechanical properties of nanocrystalline materials", *Advanced Engineering Materials*, (to be published).

[8] K. J. Kurzydłowski and B. Ralph, "The quantitative description of the microstructure of materials", *CRC Press*, Boca Raton, 1995.

[9] M. Suś-Ryszkowska, Z. Pakieła, R. Valiev, J. W. Wyrzykowski and K. J Kurzydlowski, "Mechanical properties of nanostructured iron obtained by different methods of severe plastic deformation", *Solid State Phenomena* 101, 85 (2004).

[10] A. Drużycka-Wiencek, M Woźniak and K. J. Kurzydłowski, "Morphology and properties of oxide films formed on the nanocrystalline 316L austenite steel", *Solid State Phenomena* 101, 77 (2004).

[11] A. Drużycka-Wiencek, D. Klassek and M. Suś-Ryszkowska, "New developments in nanostructuctured materials — synthesis, characterization, functionality", *Autumn School 2003 Humboldt — University of Berlin, "Severe Plastic Deformation Titanium and Stainless Steel for bio-medical applications".*